International Journal of Minerals, Metallurgy and Materials
Volume 19, Number 6, June 2012, Page 518
DOI: 10.1007/s12613-012-0589-z

Effect of welding process on the microstructure and properties of dissimilar weld joints between low alloy steel and duplex stainless steel

Jing Wang[1)], *Min-xu Lu*[1)], *Lei Zhang*[1)], *Wei Chang*[2)], *Li-ning Xu*[1)], *and Li-hua Hu*[2)]

1) Institute for Advanced Materials and Technology, University of Science and Technology Beijing, Beijing 100083, China

2) Research Institute of China National Offshore Oil Corporation, Beijing 100027, China

(Received: 21 July 2011; revised: 17 August 2011; accepted: 24 August 2011)

Abstract: To obtain high-quality dissimilar weld joints, the processes of metal inert gas (MIG) welding and tungsten inert gas (TIG) welding for duplex stainless steel (DSS) and low alloy steel were compared in this paper. The microstructure and corrosion morphology of dissimilar weld joints were observed by scanning electron microscopy (SEM); the chemical compositions in different zones were detected by energy-dispersive spectroscopy (EDS); the mechanical properties were measured by microhardness test, tensile test, and impact test; the corrosion behavior was evaluated by polarization curves. Obvious concentration gradients of Ni and Cr exist between the fusion boundary and the type II boundary, where the hardness is much higher. The impact toughness of weld metal by MIG welding is higher than that by TIG welding. The corrosion current density of TIG weld metal is higher than that of MIG weld metal in a 3.5wt% NaCl solution. Galvanic corrosion happens between low alloy steel and weld metal, revealing the weakness of low alloy steel in industrial service. The quality of joints produced by MIG welding is better than that by TIG welding in mechanical performance and corrosion resistance. MIG welding with the filler metal ER2009 is the suitable welding process for dissimilar metals jointing between UNS S31803 duplex stainless steel and low alloy steel in practical application.

Keywords: dissimilar metals; welds; stainless steel; alloy steel; microstructure; mechanical properties; corrosion

[*This work was financially supported by the National Science and Technology Major Project of China (Grant No.2011ZX05056).*]

1. Introduction

Dissimilar weldments have been widely used in the oil and gas industry because of economic benefits as well as the full advantage of outstanding performance of two different metals, such as strength and corrosion resistance. With the development of oil and gas exploitation in deepwater, more and more duplex stainless steels (DSS) have been used in the flowline; however, low alloy steels are used in the cool end flowline section for economic consideration. Therefore, dissimilar weld joints are unavoidable.

The properties of dissimilar welding joints and even the feasibility of welding processes are influenced by many factors, for example, carbon migration from the low alloy side, microstructure gradient, and different residual stress situations across different regions of weld metal [1]. Some weld defects, such as dilutions and cracks, may generate in weld metal and lead to the great decrease of weld metal properties, if the welding process is not well be controlled. Some researchers have focused on the properties of dissimilar weld joints, and many significant works were carried out on the welding behavior and mechanical properties of dissimilar welding joints [2-4]. Paventhan *et al.* [5] studied the fatigue behavior of friction-welded medium carbon steel and austenitic stainless steel dissimilar joints, and their result showed that the fatigue strength of joints was correlated with the microstructure, microhardness, and tensile properties of joints. Wang *et al.* [6] used tungsten inert gas (TIG) arc welding (GTAW) and shielded metal arc welding (SMAW) to research the characterization of microstructure,

Corresponding author: Min-xu Lu E-mail: lumx@ustb.edu.cn

mechanical properties, and corrosion resistance of dissimilar welded joints between UNS S31803 duplex stainless steel and 16MnR, and their conclusion was that, GTAW was the suitable welding process for joining dissimilar metals between UNS S31803 DSS and 16MnR. However, the effect of welding process on the properties of dissimilar weld joints between DSS and low alloy pipeline steel has seldom been studied.

To obtain high-quality dissimilar weld joints, it was important to study the effect of welding process on the microstructure, mechanical properties, and corrosion resistance of dissimilar weld joints. The joints of dissimilar metals between DSS and low alloy steel were welded by metal inert gas (MIG) welding and TIG welding in this article. The microstructure, mechanical properties, and corrosion behavior of dissimilar weld joints were investigated by scanning electron microscopy (SEM), tensile test, low temperature impact test, microhardness measurement, and polarization technique.

2. Experimental

Base metals employed in this paper are low alloy steel (API X70) and DSS (UNS S31803), and their chemical composition is given in Table 1. The base metals are machined to the dimension of 200 mm×100 mm×8 mm, and a single groove is prepared with an angle of 60°. The schematic of a weld joint is shown in Fig. 1. Joints are carried out by two different types of welding processes, which are MIG welding and TIG welding with ER2209 welding wires. The welding parameters are summarized in Table 2.

Table 1. Chemical composition of base metals and filler metal **wt%**

Material	C	Si	Mn	P	S	Cr	Ni	Mo	Nb	Cu	N
API X70	0.055	0.20	1.52	0.008	0.0007	0.031	0.22	0.21	0.033	0.21	0.22
UNS S31803	0.014	0.39	1.38	0.023	0.0010	22.39	5.68	3.13	0.006	0.18	0.17
ER2209	0.040	0.51	1.55	0.018	0.0150	22.92	8.61	3.12	—	—	0.17

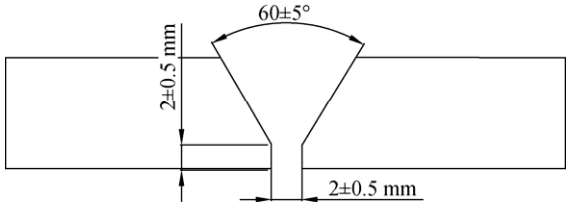

Fig. 1. Welding groove.

Table 2. Welding parameters

Welding technology	Welding current / A	Electric voltage / V	Welding speed / (mm·min^{-1})	Heat input / (kJ·mm^{-1})
TIG	120	20-22	30-35	1.0
MIG	280	23-25	50-60	2.5

Mechanical properties tests and microstructural analyses were conducted after welding. The weld metal and UNS S31803 DDS base metal were etched by aqua-regia, and X70 base metal was etched by a 5wt% natal solution. Microstructural features were observed by optical microscopy and SEM. Energy-dispersive spectroscopy (EDS) was employed for chemical analysis in different zones of weldments. Mechanical properties tests of weld joints included microhardness measurement, tensile test, and impact test. Samples of impact test were performed with the sub-size dimension of 55 mm×10 mm×5 mm at –40°C. Pitting corrosion resistance was measured by FRA PASTAT 2273 electrochemical station in a 3.5wt% NaCl solution at ambient temperature. Polarization curves were recorded *via* the three-electrode cell by using a Pt foil as the auxiliary electrode and a saturated calomel electrode as the reference electrode. The experiments were performed at a scan rate of 0.5 mV/s. In the period immersing test, weld metals (WM) were immersed in artificial deepwater (4°C) for 30 d, and the composition of artificial deepwater is shown in Table 3.

Table 3. Composition of artificial deepwater **g/L**

NaCl	Na_2SO_4	KCl	$NaHCO_3$	KBr	H_3BO_3	$MgCl_2·6H_2O$	$CaCl_2·2H_2O$
23.926	4.008	0.667	0.196	0.098	0.026	0.053	0.010

3. Results and discussion

3.1. Microstructure

The microstructures of DSS (UNS S31803) and low alloy steel (API X70) are shown in Fig. 2. Austenite phase in DSS base metal is embedded in the ferrite matrix (gray area) with nearly equal amounts of ferrite, while the microstructures of X70 steel reveal a mixture of acicular ferrite and pearlite.

The optical micrographs of microstructures across the heat-affected zone (HAZ) from the fusion zone to DSS base metal are shown in Figs. 3(a) and (b). Austenite grains appear firstly along the grain boundary, and small grains exist in the interior of the ferrite grain in the process of melting and rapid cooling. As a result, the typical characteristics of dendritic structure with fine crystals and big intercrystalline areas are formed; meanwhile, some crystals appear as Widmanstatten in the weld metal, which are detrimental to resist crack propagation. Compared with the base metal, the increase of austenite appeared in the weld metal due to the use of the filler metal with a high content of nickel.

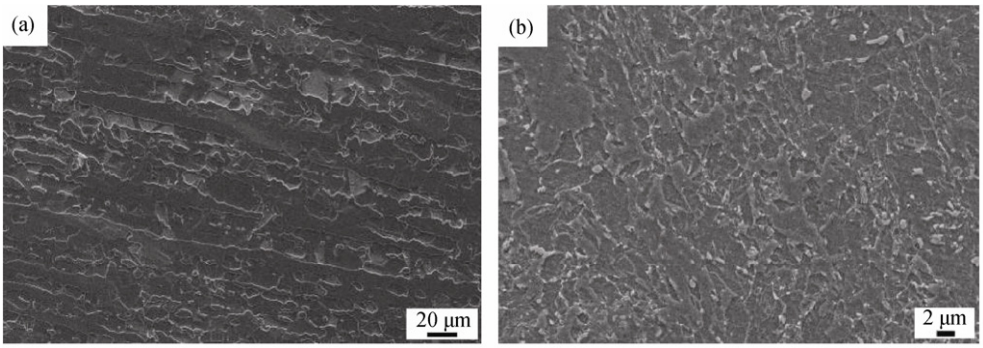

Fig. 2. SEM images of UNS S31803 (a) and API X70 (b).

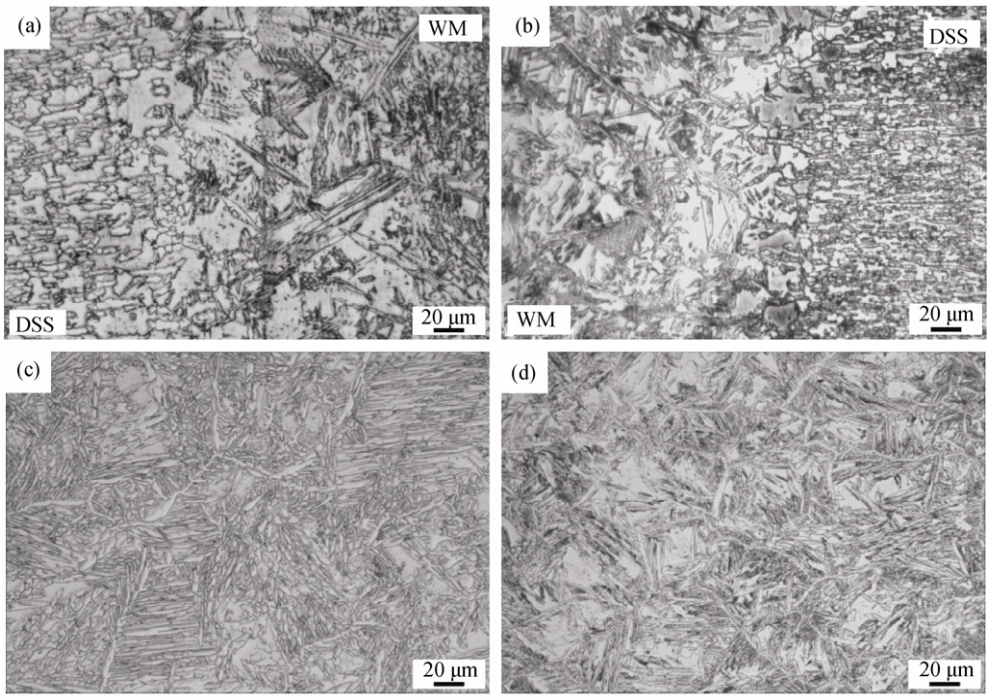

Fig. 3. Microstructures of DSS in HAZ and weld metal (WM): (a) DSS in HAZ by MIG; (b) DSS in HAZ by TIG; (c) WM by MIG ; (d) WM by TIG.

The two weld metals show similar microstructural features characterized by large ferrite grains with intragranular and intergranular austenite, as shown in Figs. 3(c) and (d). More austenite is formed in the weld metal of MIG welding due to its slower cooling rate.

Microstructural features and EDS curves at interfaces between X70 and the weld metal are shown in Fig. 4. The type II boundary characteristic of dissimilar weld joints is observed in parallel with the fusion boundary at the side of X70 steel. The type II boundary was usually the fracture path observed by many investigators [7-8]. The development of such a boundary was attributed to differences in crystal structure between the materials being joined, the diffusional mixing of alloy and impurity elements from the weld metal into a stagnant boundary, and the change of base metal dilution, which affected the composition gradient in the weld metal [9]. Different widths of fusion zones observed in the weld metal were relative to the different heat

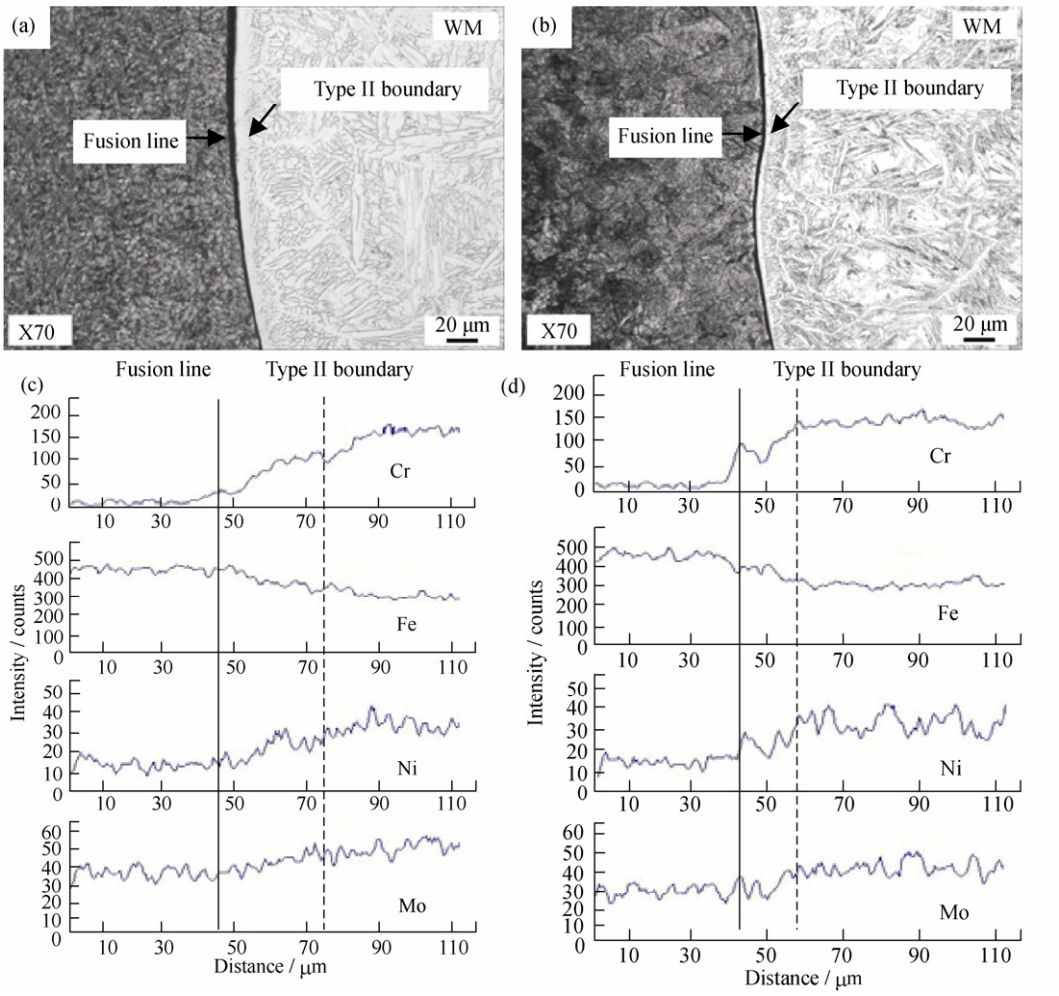

Fig. 4. Microstructures and EDS curves of X70 steel in HAZ and weld metal: (a) SEM image by MIG; (b) SEM image by TIG; (c) EDS spectrum by MIG; (d) EDS spectrum by TIG.

inputs and cooling rates. A slower cooling rate of MIG welding resulted in a wider fusion zone than TIG welding, which was beneficial to resist hydrogen-induced cracking. In X70 HAZ closed to the fusion line, there is a coarse grain zone, and a narrower one appears in MIG welding, which may be caused by the higher heat input.

EDS spectra performed in weldments reveal chemical transition from the fusion boundary across the type II boundary regions. Concentration gradients of Cr and Ni exist between X70 steel and the weld metal. The concentration of Cr decreases markedly around the fusion line, while the concentration of Ni varies slowly. The diffusion of carbon from the X70 side into the weld metal, the diluting effect of X70 steel, and the fast cooling of the molten pool led to alloy element gradients near the fusion line [10].

3.2. Mechanical properties

The tensile properties of the two weld metals are reported in Table 4. Locations of fracture are all at the side of X70 base metal. Tensile strength values of the two weld metals are all around 640 MPa.

Table 4. Tensile properties of weld metal

Welding technology	Tensile strength / MPa	Extension strength / MPa	Elongation rate / %
TIG	646.24	487.34	16.67
MIG	638.07	458.97	16.33

A higher hardness is observed in the narrow zone between the fusion boundary and type II boundary, as seen in Fig. 5, which may be caused by the formation of harder microconstituents (martensite/carbides), owing to carbon migration from the X70 side.

The impact strengths of DSS base metal (DSS BM), X70 in HAZ, X70 base metal (X70 BM), and the two weld metals are tested at –40°C, as presented in Fig. 6. DSS base

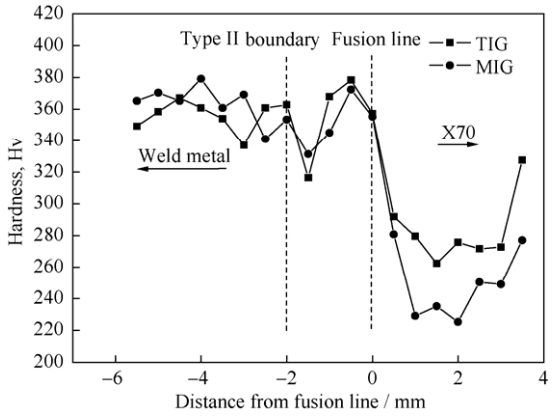

Fig. 5. Hardness distribution of weld metal.

metal and the weld metals show the higher toughness because of high austenite content, and well-distributed austenite and ferrite make DSS base metal present the highest toughness. The toughness of X70 in HAZ exhibits a lower impact strength than that of the base metal, which is relation to coarse grains in this zone. The impact toughness of MIG welding is higher than that of TIG welding in the weld metal. More austenite phases generate during MIG welding due to the decrease of ferrite-to-austenite transformation ratio with the increase of heat input and slower cooling rate [11].

The fracture morphology of Charpy impact samples at –40°C is shown in Fig. 7. As the ductile-brittle transition temperature of DSS is lower than –50°C, DSS base metal shows a ductile fracture with a dimpled structure in Fig. 7(a). Fig. 7(b) is the fracture feature of X70 steel, in which brittle cleavages appear. The fracture features of TIG weld metal and MIG weld metal are presented in Figs. 7(c) and (e). Compared with TIG weld metal, much more dimples distribute in MIG weld metal evenly, which have more austenite and phase boundaries [12]. More crystal boundaries of X70 in HAZ by MIG welding are shown in Fig. 7(f), which correspond to much more fine crystals in Fig. 4(a).

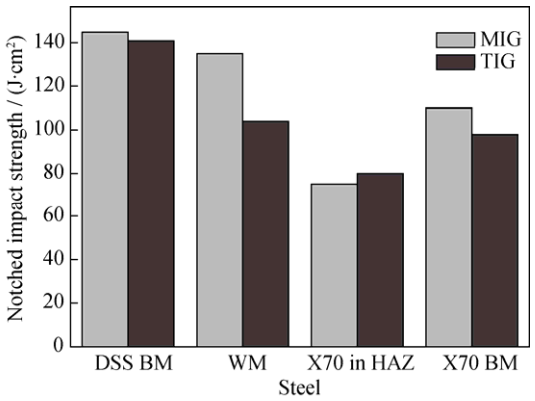

Fig. 6. Impact strength of DSS base metal (DSS BM), X70 in HAZ, X70 base metal (X70 BM), and two weld metals at –40°C.

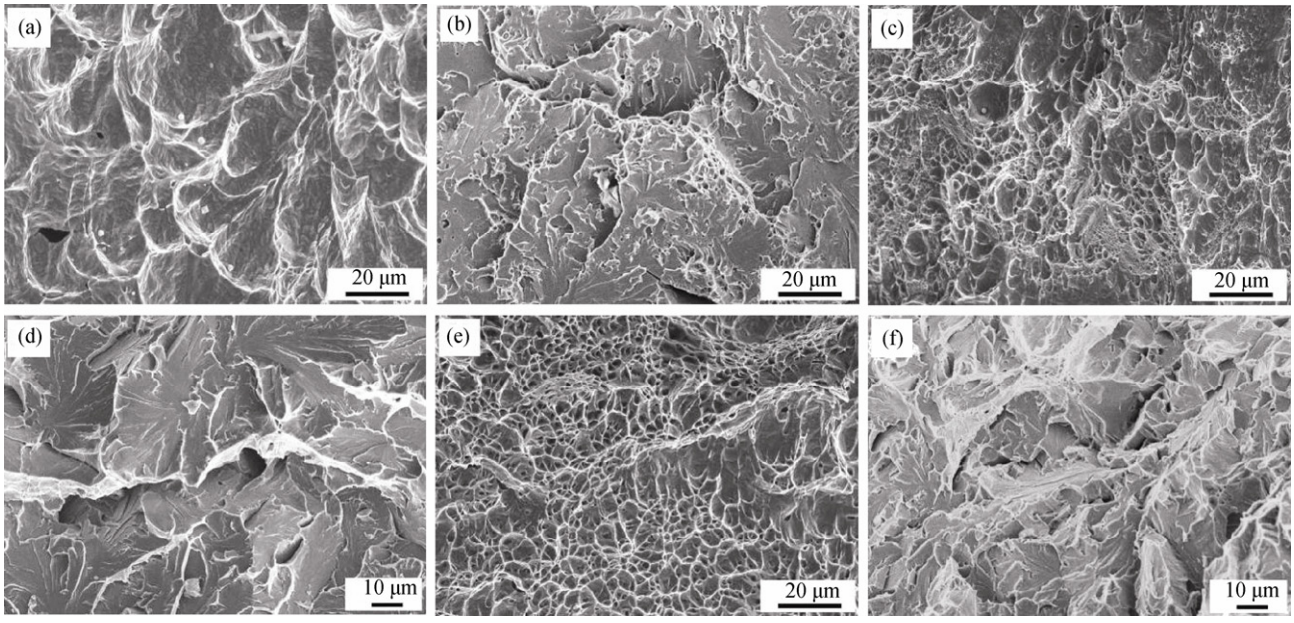

Fig. 7. Fracture morphology of Charpy impact samples: (a) DSS base metal; (b) X70 base metal; (c) TIG weld metal; (d) X70 in HAZ by TIG; (e) MIG weld metal; (f) X70 in HAZ by MIG.

3.3. Corrosion resistance

The polarization curves of the base metals, X70 in HAZ, and the weld metals in a 3.5wt% NaCl solution at ambient temperature are depicted in Fig. 8. Since DSS in HAZ is

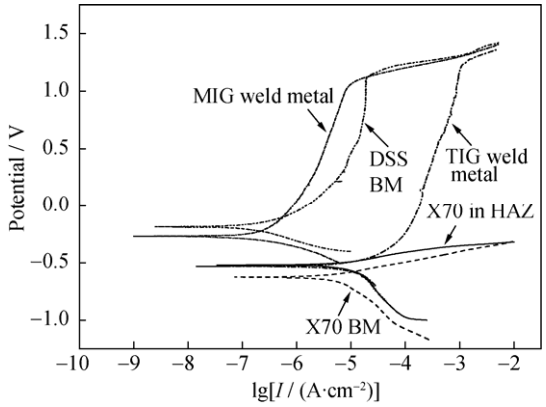

Fig. 8. Polarization curves of different regions of dissimilar weldments in a 3.5wt% NaCl solution.

very narrow, its corrosion behavior is ignored. The results show that DSS base metal and the weld metal have the higher corrosion potential. The corrosion current density (I) of TIG weld metal is higher than that of MIG weld metal in a 3.5wt% NaCl solution, indicating that MIG weld metal has high resistance to seawater. Compared with DSS, the corrosion potential of X70 base metal and X70 in HAZ are lower obviously, and X70 in HAZ shows a higher corrosion potential than that of X70 base metal.

The microscopic morphology of the weld metal after immersion for 30 d in artificial deepwater at 4°C is shown in Fig. 9. Compared with slight corrosion in the weld metal, severe corrosion appears in the HAZ of X70 steel. Loose corrosion products cover on the surface of HAZ, and the element analysis of corrosion products of X70 steel in HAZ is shown in Table 5. The result shows that iron oxide and little chromium oxide are occupied in the HAZ of X70. Different potentials between X70 steel and the weld metal leads to galvanic corrosion, which results in severe corrosion in X70 steel. It reveals that X70 base metal is weak in industrial service.

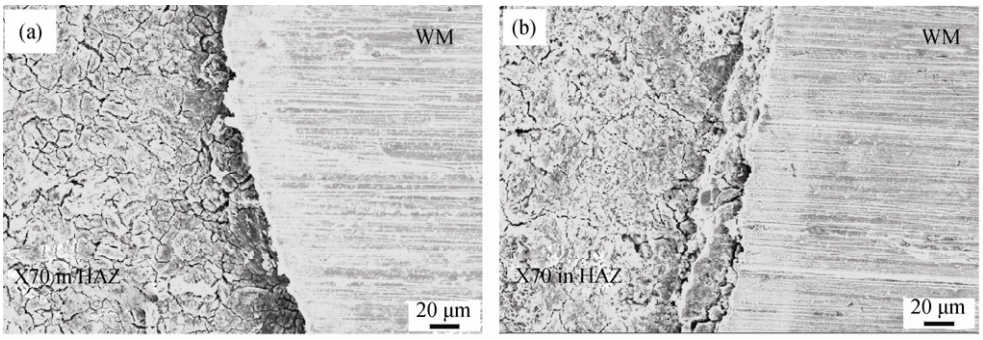

Fig. 9. Microscopic morphology of the weld metal after immersion for 30 d in artificial deepwater at 4°C: (a) MIG; (b) TIG.

Table 5. Element distribution of X70 steel in HAZ

Element	Weld metal		X70 in HAZ	
	Content / wt%	Content / at%	Content / wt%	Content / at%
Fe	74.62	73.88	74.63	49.45
Cr	17.57	18.69	0.00	0.00
O	0.00	0.00	20.77	48.04
Mo	1.89	1.09	2.92	1.13
Ni	5.16	4.86	0.39	0.00
Si	0.75	1.49	0.00	0.52
Mn	0.00	0.00	1.29	0.87

4. Conclusions

(1) More austenite presents in the weld metal by MIG welding than that by TIG welding, and the austenite content increases obviously in the weld metal compared with DSS base metal, which is beneficial to mechanical properties and corrosion resistance.

(2) The type II boundary is observed on the weld metals, which are closed to the fusion boundary at the side of X70 steel. Obvious concentration gradients of Ni and Cr exist between the fusion boundary and the type II boundary. A lower cooling rate of MIG welding results in a wider fusion zone than TIG welding, which is beneficial to resist hydrogen-induced cracking.

(3) Tensile strength values of the weld metals are all around 640 MPa. The toughness of the weld metal is lower than that of DSS base metal, while the impact toughness of MIG welding is higher than that of TIG welding in the weld metal. The fracture feature of DSS base metal and the weld metal are ductile.

(4) The current density of TIG weld metal is higher than that of MIG weld metal in a 3.5wt% NaCl solution, indicating that MIG weld metal has high resistance to seawater. Galvanic corrosion between X70 steel and the weld metal results in severe corrosion in X70 steel, which reveals the weakness of X70 base metal in industrial service.

(5) The mechanical properties and corrosion resistance of MIG weld metal are prior to TIG weld metal. MIG welding with filler metal ER2009 is the suitable welding process for dissimilar metals jointing between UNS S31803 DSS and X70 in practical application.

References

[1] Z. Sun and R. Karppi, The application of electron beam welding for the joining of dissimilar metals: an overview, *J. Mater. Process. Technol.*, 59(1996), No.3, p.257.

[2] M.K. Samal, M. Seidenfuss, E. Roos, and K. Balani, Investigation of failure behavior of ferritic-austenitic type of dissimilar steel welded joints, *Eng. Failure Anal.*, 18(2011), No.3, p.999.

[3] G. Phanikumar, K. Chattopadhyay, and P. Dutta, Joining of dissimilar metals: issues and modeling techniques, *Sci. Technol. Weld. Joining*, 16(2011), No.4, p.313.

[4] H. Naffakh, M. Shamanian, and F. Ashrafizadeh, Dissimilar welding of AISI 310 austenitic stainless steel to nickel-based alloy Inconel 657, *J. Mater. Process. Technol.*, 209(2009), No.7, p.3628.

[5] R. Paventhan, P.R. Lakshminarayanan, and V. Balasubramanian, Fatigue behaviour of friction welded medium carbon steel and austenitic stainless steel dissimilar joints, *Mater. Des.*, 32(2011), No.4, p.1888.

[6] S.G. Wang, Q.H. Ma, and Y. Li, Characterization of microstructure, mechanical properties and corrosion resistance of dissimilar welded joint between 2205 duplex stainless steel and 16MnR, *Mater. Des.*, 32(2011), No.2, p.831.

[7] T.W. Nelson, J.C. Lippold, and M.J. Mills, Nature and evolution of the fusion boundary in ferritic-austenitic dissimilar weld metals: Part 1. Nucleation and growth, *Weld. J.*, 78(1999), No.10, p.329.

[8] T. Hattori, T. Fujita, K. Kinoshita, A. Ebata, H. Tsukamoto, and M. Ando, Hydrogen induced disbonding of stainless steel overlay weld and its preventive measures, *Nippon Kokan Tech. Rep. Overseas*, 47(1986), p.17.

[9] T.W. Nelson, J.C. Lippold, and M.J. Mills, Nature and evolution of the fusion boundary in ferritic-austenitic dissimilar metal welds: Part 2. On-cooling transformations, *Weld. J.*, 55(2000), No.10, p. 267.

[10] P. Bala Srinivasan, V. Muthupandi, W. Dietzel, and V. Sivan, Microstructure and corrosion behavior of shielded metal arc-welded dissimilar joints comprising duplex stainless steel and low alloy steel, *J. Mater. Eng. Perform.*, 15(2006), No.6, p.758.

[11] R. Badji, M. Bouabdallah, B. Bacroix, C. Kahloun, B. Belkessa, and H. Maza, Phase transformation and mechanical behavior in annealed 2205 duplex stainless steel welds, *Mater. Charact.*, 59(2008), No.4, p.447.

[12] K. Migiakis and G.D. Papadimitriou, Effect of nitrogen and nickel on the microstructure and mechanical properties of plasma welded UNS S32760 super-duplex stainless steels, *J. Mater. Sci.*, 44(2009), No.23, p.6372.